Geomicrobiology Journal, 25:228–239, 2008

ISSN: 0149-0451 print / 1521-0529 online
DOI: 10.1080/01490450802153462

Evaluation of Electron Microscopic Sample Preparation Methods and Imaging Techniques for Characterization of Cell-Mineral Aggregates

S. Schädler
Geomicrobiology Group, Center for Applied Geosciences, University of Tuebingen, Germany

C. Burkhardt
NMI Natural and Medical Sciences Institute at the University of Tuebingen, Germany

A. Kappler
Geomicrobiology Group, Center for Applied Geosciences, University of Tuebingen, Germany

Scanning Electron Microscopy (SEM) is used to image geomicrobiological samples, typically containing interfaces between "hard and soft materials" such as minerals and cells, which represent challenges for artifact-free preparation for high-resolution imaging. We used cell-mineral aggregates produced during microbial Fe(II) oxidation and Fe(III) reduction to evaluate different sample preparation and imaging techniques. Both rapid freezing and standard critical point drying (CPD) preserve structures of geomicrobiological samples, at least the ones obtained for Fe(II)-oxidizing and Fe(III)-reducing bacteria, without artifacts. We recommend a SEM sample preparation scheme for geomicrobiological specimens and discuss critical parameters like fixation, dehydration, coating, and acceleration voltages.

Keywords scanning electron microscopy, geomicrobiology, cell-mineral interactions, iron oxidation, reduction

INTRODUCTION

Bacteria typically attach to solid surfaces, forming biofilms in order to establish a protected neighborhood, to sequester nutrients and to utilize cooperative benefits of microbial communities (Jefferson 2004; Kolter and Greenberg 2006). The surfaces of redox-active minerals, such as Fe(II) and Fe(III) minerals, also represent such environments and can even be involved in microbial energy metabolism by providing (e^--donor) or accepting (e^--acceptor) electrons (Kappler and Straub 2005; Weber et al. 2006). By changing the redox state of metals via electron transfer and by changing the pH of their surrounding environment, bacteria can dissolve and precipitate solid phases. In the environment this can have implications for processes such as mineral dissolution, corrosion of metals and changes in groundwater chemistry potentially leading to drinking water problems (Ehrlich 1996; Konhauser 2006).

During Fe(III) reduction (Nealson and Saffarini 1994; Lovley et al. 2004; Hansel et al. 2005) and aerobic (Emerson and Weiss 2004) and anaerobic (Widdel et al. 1993; Straub et al. 1996) Fe(II) oxidation, iron minerals are formed, transformed and dissolved. Samples that contain close associations of minerals and cells are formed (Fortin and Ferris 1998). The mechanisms of how microorganisms deal with the poor solubility of their substrates or metabolic products, e.g., the Fe(III) produced during Fe(II) oxidation at neutral pH, are still poorly understood and only high-resolution imaging and analysis techniques can provide better insights. Scanning electron microscopy (SEM) is widely used for the imaging of surfaces (Brown et al. 1998; Erlandsen et al. 2003; Kappler et al. 2005; Fortin and Langley 2005) and can, when used in studies that change systematically environmental parameters, help to obtain insights into the mechanisms of mineral precipitation and dissolution, as well as the mechanisms of the cell-mineral interactions.

However, the close associations of solid particles (minerals) and "soft & wet" material (biomass) represent a challenge for obtaining high resolution images of non-disturbed structures. During imaging, the specimens are kept in a high vacuum where, in a wet biological sample, water evaporation, and thus cell deformation or even cell lysis would occur. Therefore, these samples either need to be dried beforehand or rapidly frozen and

Received 5 October 2007; accepted 21 April 2008.
Author Schadler is also affiliated with NMI, Tuebingen. This work was supported by an Emmy-Noether fellowship and several research grants from the German Research Foundation to Andreas Kappler, and by a BMBF research grant (13N8652) to the Natural and Medical Sciences Institute at the University of Tuebingen. We would like to thank F. Hegler, P. Larese-Casanova, N. Posth, U. McKnight and M. Scherer, and three anonymous reviewers for their helpful comments improving the manuscript.
Address correspondence to Andreas Kappler, Geomicrobiology Group, Center for Applied Geosciences, University of Tuebingen, Sigwartstrasse 10, D-72076 Tübingen, Germany. E-mail: andreas.kappler@uni-tuebingen.de

then kept at very low temperatures during imaging. Samples are often dried by making use of the critical point phenomenon (Anderson 1950). This technique requires stepwise fixation and dehydration procedures.

Since biological samples are usually neither highly conductive nor very electron dense, a metal or carbon coating is applied in many cases in order to increase the conductivity and electron density and to facilitate imaging. These sample preparation steps (e.g., fixation, dehydration and coating) can potentially cause artifacts such as cell shrinkage during dehydration, surface alterations, formation of secondary minerals by chemical oxidation of O_2-sensitive components during fixation and formation of associations of components that were not associated in the original sample. All of these artifacts may mislead the interpretation of results regarding the native state of the samples before the preparation.

Despite the widespread use of SEM for analysis of geomicrobiological samples (typically consisting of a mixture of "hard and soft" materials such as minerals and cells), many publications give only very limited information about the details of SEM sample preparation, which makes it difficult to repeat and compare experiments. Additionally, it is usually not stated why a certain SEM technique (cryo-SEM, SEM, Environmental SEM), sample preparation protocol (e.g., dehydration procedure, sample coating), detector (e.g., in-lens detector, secondary electron detector, backscattered electron detector) and imaging parameters (acceleration voltage, working distance) were chosen.

The goals of this study therefore were (i) to evaluate whether and which kind of artifacts are created during different steps of preparation of geomicrobiological samples for the analysis of surfaces in the SEM and (ii) to recommend a sample preparation scheme for routine imaging of a large number of geomicrobiological samples by SEM. For this purpose, three strains of Fe(II)-oxidizing and Fe(III)-reducing bacteria were chosen for the evaluation and direct comparison of different preparation and imaging methods.

The use of wet or environmental scanning electron microscopy (ESEM) (Thiel 2006) would be an alternative to the elaborate and time-consuming sample preparation techniques required for SEM (fixation, dehydration, coating), since ESEM allows for the imaging of samples under hydrated conditions without any further treatment. However, we do not evaluate this technique in this study as previous ESEM studies did not report sufficiently high resolutions (in the size range of a few tens of nanometers) required for the evaluation of spatial relationships of microbial cells with mineral particles (Thiberge et al. 2004; Hammel and Anaby 2007).

MATERIALS AND METHODS

Bacterial Strains

For this study the following anoxygenic phototrophic Fe(II)-oxidizing bacteria from our own culture collection were used: the purple sulphur bacterium *Thiodictyon* sp. strain F4 and the green sulphur bacterium *Chlorobium ferrooxidans* sp. strain KoFox. The Fe(III)-reducing organism *Shewanella oneidensis* strain MR-4 was kindly provided by Dr. J. Gralnick (University of Minnesota, USA).

Growth Medium and Cultivation Conditions

Phototrophic Fe(II)-oxidizing strains were cultivated in a freshwater mineral medium and either dissolved Fe(II), hydrogen or acetate was utilized as an electron donor at pH 6.8–7.0, as described previously (Kappler and Newman 2004). Cultures were incubated at 20°C and light saturation (>700 lux). Fe(II) oxidation was followed by spectrophotometrical quantification of the remaining Fe(II) (ferrozine assay) in the cultures as described previously (Kappler and Newman 2004). Fe(II) oxidation data was used to collect and investigate microbial cells at similar and reproducible growth status of the cells, but is not shown in this study. For growth data of the strains used in this study, see e.g., Kappler and Newman (2004).

A frozen stock culture of *Shewanella oneidensis* strain MR-4 was kept at −80°C and streaked out on LB-agar plates. LB-medium contained (per 1 L of Millipore H_2O): 10 g tryptone, 5 g yeast extract, 5 g NaCl and 12 g agar (not added for liquid cultures). LB-plates were incubated at 28°C for approximately 24 h and kept at 4°C for up to 10 days. For liquid culture preparation, 50 mL of liquid LB medium in a 200 mL Erlenmeyer flask were inoculated with a single colony isolated from the LB-plate. The flask was covered with aluminium foil and incubated at 28°C, at 150 rpm on a rotary shaker. Cells were harvested after 14 h to prepare the inoculum for experiments. Then, 2 mL culture were withdrawn and centrifuged (5 min, 10 000 g). Cells were washed twice with LML-medium, resuspended in 2 mL of medium and diluted to a final concentration of $2*10^5$ cells/mL. Cells were added to the cultivation tubes after the medium and all other substrates were added.

LML-medium (Myers and Myers 1994), containing 12 mM HEPES buffer and 30 mM sodium lactate set to pH 7, was prepared anoxically using a Widdel flask. Once the medium had cooled to 80°C, it was removed from the autoclave (121°C, 25 min) and the headspace was exchanged with N_2 for 5 min. Afterward, the medium was cooled to approximately 22°C and filled into 50 mL screw cap bottles for storage. Ferrihydrite (Fe(III) hydroxide 5 mM, synthesized according to Schwertmann and Cornell (2000)) was added as a substrate and the cell suspension was added with a syringe.

Sampling

For the preparation of samples for electron microscopic analyses, 1 mL aliquots were sampled from the culture bottles with a N_2/CO_2-flushed syringe under sterile conditions. Samples were taken at the late exponential growth phase, when iron was almost completely oxidized (in the case of Fe(II)-oxidizing strains) or reduced (in the case of Fe(III)-reducing strains). Samples in 1 mL Eppendorf tubes were then further prepared for critical point drying.

For cryo-electron-microscopy-experiments, TEM grids (holey carbon coated, 200 mesh) were added directly into the medium bottles for microbial colonization (the grids were added to the bottles prior to autoclaving in order to guarantee sterile conditions). These bottles were opened in order to recover the grid, which was then further processed either for critical point drying or cryo-immobilization.

Critical Point Drying

Samples for critical point drying were chemically fixed in mixtures of formaldehyde and glutaraldehyde at concentrations between 1% (vol/vol) and 10% (vol/vol) in phosphate buffered saline, PBS (Dulbecco's PBS, H31-002 from PAA, Pasching, Austria), by adding fixative solution to 1 mL aliquots. Samples were then centrifuged (5,000 g), Supernatant removed, and pellet resuspended in 200 μl of PBS and pipetted on TEM grids (holey carbon coated, 200 mesh). After transfer to the grids, they were washed twice with PBS and twice with bi-distilled water, dehydrated either in microtiter plate wells or directly in droplets of dehydrating solvent on an inert parafilm surface in subsequent steps of increasing organic solvent (ethanol, acetone or isopropanol) concentrations (0, 15, 30, 50, 70, 80, 90, 96, 100, 100, 100% vol/vol) and transferred to the Critical Point Dryer Bal-Tec CPD 030.

The solvent was replaced by liquid CO_2 at a pressure of 50 bar and a temperature of 8°C. After complete replacement of the organic solvent by CO_2, the chamber was heated resulting in an increased pressure due to evaporating CO_2. Two minutes after reaching the critical point, the pressure was released very slowly, resulting in a dry sample surrounded by CO_2 at ambient pressure and temperature. Dry samples were mounted on aluminum stubs using double-sided carbon tape. For enhanced electrical conductivity, the edges of the TEM grids were painted with conductive silver paste.

Coating

Critical point dried samples were rotary coated in a Balzers sputter coater SCD 40 (Bal-Tec, Balzers, Liechtenstein) with Au/Pd (90%/10% w/w) under an angle of 45°. The coating thickness was approximately 20 nm (determined in Focused Ion Beam cross-sections and by a surface texture analyzer, results not shown). Cryo-immobilized samples were Tungsten coated unidirectionally in the Bal-Tec cryo sputter coater SCD 500 with a layer thickness of ~5 nm.

Cryo-Immobilization

TEM grids were taken out of the microbial cultures and washed in bi-distilled water. Excess water was removed by touching the center of the grid with a fine filter paper from below (leading to water suction through the grid pores). Grids were immediately immersed into liquid nitrogen in a Bal-Tec cryo system (Bal-Tec VCT 100 and cryo sputter coater SCD 500). Right after plunge freezing, the grids were first transferred to the sample holder within liquid nitrogen, and then to the scanning electron microscope in a cooled shuttle that contained a nitrogen atmosphere to avoid precipitation of moisture on the sample during transfer, and imaged at temperatures below −120°C. If necessary, samples were freeze-etched for 5 min at −90°C and coated with a tungsten layer of approximately 5 nm thickness.

Electron Microscopy

The specimens were imaged in a Zeiss Gemini 1550VP FE-SEM and a Zeiss Gemini 1540XB FIB/FE-SEM equipped with a Bal-Tec cryo transfer system VCT 100 (cooled sample stage and shuttle lock). Both microscopes are equipped with Everhart-Thornley SE detectors and in-lens detectors and optimized to a lens aperture of 30 μm, which was therefore utilized in this study. Images were recorded in a format of 1024 × 768 pixels, at integration times between 15 μs and 45 μs per pixel. Plunge-frozen samples were kept at −140°C during imaging.

RESULTS AND DISCUSSION

We evaluated different methods for the artifact-free preparation of geomicrobiological samples for scanning electron microscopy (where "artifact-free preparation" refers to the sample surfaces and not the intracellular, structural details). Based on this work, we recommend a sample preparation scheme for the SEM imaging of geomicrobiological samples (Table 1,

TABLE 1
Sample preparation and imaging parameters that yielded the best results for the geomicrobiological samples analyzed in this study

Preparation step	Chemical, concentration/ material	Application time
Chemical fixation	Mixture of 2% glutaraldehyde and 4% formaldehyde in PBS	30 min*
Dehydration	Isopropanol at 10, 30, 50, 70, 80, 90, 96, 100, 100%	20 sec*
Dehydration, last step	Isopropanol 100%**	20 min*
Coating	Au/Pt 90%/10% w/w (CPD samples, W (cryo-fixed samples)	
Imaging Parameters	Recommended setting	
Acceleration Voltage	<1 kV***	
Working Distance	<1 mm***	

*Application times are strongly dependent on the sample size.
**Isopropanol dried on molecular sieve.
***Imaging parameters depend on the microscope and the combination of microscope, detectors, and sample.

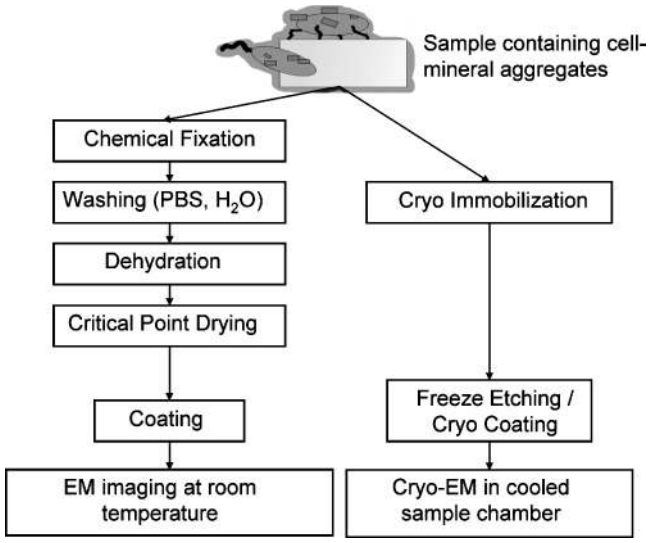

FIG. 1. Schematic representation of the different protocols used for sample preparation for scanning electron microscopy (SEM). Critical point drying allow imaging at room temperature. Cryo-immobilization without freeze-drying requires cooled microscope sample stages.

Figure 1). We focused on samples of phylogenetically and morphologically different strains of Fe(II)-oxidizing bacteria that produce Fe(III) minerals during their metabolism, forming aggregates of cells and Fe(III) minerals. Additionally, we analyzed cell-mineral aggregates formed during microbial reduction of Fe(III) hydroxides. For the preparation of these samples for electron microscopical imaging, conventional critical point drying (CPD) of chemically fixed and dehydrated cells (Figure 1, left), as well as a rapid freezing method (plunge freezing, also termed cryo-immobilization, Figure 1, right) were applied, and coated samples were compared to non-coated samples.

After evaluating the sample preparation methods and comparing traditional methods (CPD) to cryo-immobilization, we varied the imaging methods and imaging parameters, including detectors, sample coating, working distances, acceleration voltages and integration times, in order to determine the optimal microscope settings for the imaging of samples containing cell-mineral aggregates.

Preparation of Geomicrobiological Samples for Scanning Electron Microscopy via Chemical Fixation, Dehydration, and Critical Point Drying

Due to the high vacuum ($\sim 10^{-6}$ mbar) in SEM sample chambers, the water that is usually present in geomicrobiological samples (culture medium, water in the microbial cells, etc.) would vaporize at room temperature thereby leading to the collapse of biological material, i.e., cell lysis. One method to avoid this is to lower the vapor pressure by keeping the samples and the microscope at a very low temperature, as described below. The most common way to avoid evaporation is the stepwise replacement of water from the sample first by an organic solvent (e.g., ethanol) and then by liquid CO_2, which is brought to the hypercritical state and thus evaporates without a direct phase transition. This method is frequently used for sample preparation and consists of three basic steps: (i) chemical fixation of the biological structures, (ii) dehydration by organic solvents and (iii) critical point drying (CPD).

Liquid CO_2 is used for the final drying of the sample since the critical point of CO_2 is conveniently reached using simple lab techniques (about 31°C and 74 bar, unlike the critical point of water: 374°C and 220 bar). Preceding this step, however, an organic solvent, e.g., ethanol, is used to dehydrate the sample, as water and CO_2 are not completely miscible. Organic solvents would also denaturize the biologic tissue; therefore, a chemical fixation of cell material is needed to precede the dehydration. In order to optimize the sample preparation protocol, we evaluated the three steps, i.e., chemical fixation, dehydration by organic solvents and critical point drying.

Sample Preparation Step I: Chemical Fixation of Microbial Cells Prior to Dehydration. Formaldehyde, glutaraldehyde (Sabatini et al. 1963) and mixtures of both fixatives (Karnovsky 1965; Kiernan 2000) have proven to be best suited for cell preservation with few artifacts. Therefore, we exclusively used these two chemicals for the evaluation of fixative concentrations ranging from 1% to 10%, and fixation times spanning from 10 minutes to 4 hours. Post-fixation or staining by the highly toxic osmium tetroxide was not evaluated.

Formaldehyde fixation of biological specimens is a fast but reversible process, whereas application of glutaraldehyde takes more time but results in an irreversible fixation. Our experiments showed that sequential fixation using formaldehyde in a first, and glutaraldehyde in a second step (each step taking 30 min) did not result in any difference in cell preservation, compared to fixation for 30 min by a mixture of the two solutions (Figures 2a and 2b). Consequently, for further experiments, the two fixatives were used as a mixed solution in concentrations of 2% glutaraldehyde in 4% formaldehyde, as suggested by Karnovsky (1965).

While there is no difference in the cell preservation when cells are sequentially or simultaneously fixed with formaldehyde and glutaraldehyde, cells do show formation of dents and bumps when the critical point drying is omitted and the samples are only air-dried after chemical fixation (Figure 2c). Cells that were not fixed yielded SEM images in which cells were no longer present, possibly due to cell lysis or to the removal of cells by washing (not shown). Visual observation in scanning electron micrographs showed no differences in iron mineral appearance between fixed and untreated samples (not shown) suggesting no significant formation of secondary minerals by fixation.

Additionally, we found that fixation times significantly shorter than 30 min resulted in more than 50% of shrunk cells after CPD (not shown). This was especially the case for the cells of the vacuole-containing purple-sulphur bacterium *Thiodictyon* sp. strain F4. Fixation times longer than 30 min increased the preservation of cells for strain F4, leading to a smaller fraction

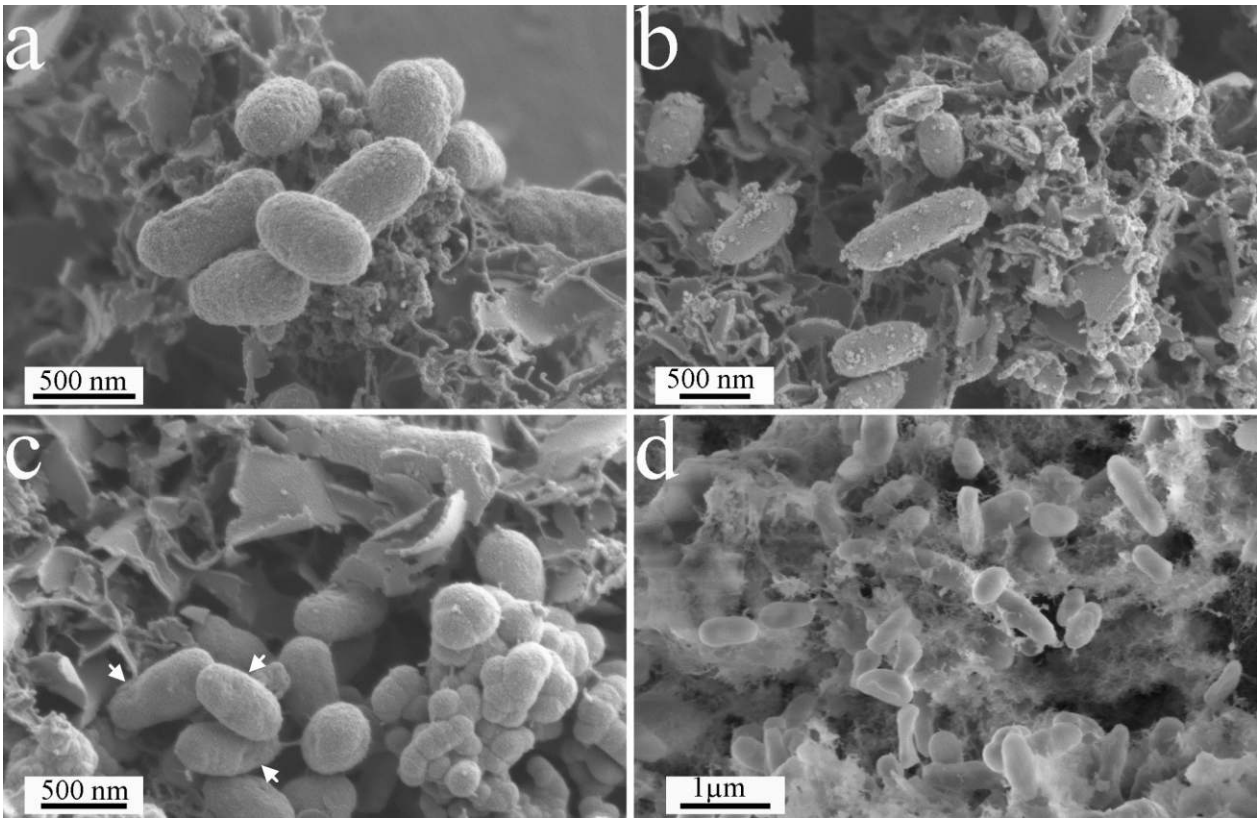

FIG. 2. Preservation of cells of the Fe(II)-oxidizing green sulphur bacterium *Chlorobium ferrooxidans* sp. strain KoFox associated with Fe(III) minerals after different preparation schemes. Images (a) and (b) show cells after critical point drying procedure. Figure (a): cells fixed with formaldehyde and glutaraldehyde in two subsequent steps. Figure (b): cells fixed with a mixture of both fixatives. Figure (c): cells after fixation with a mixture of both fixatives and subsequent air-drying. Figure (d): cells after cryo-fixation, imaging at −145°C. Imaging parameters: Acceleration voltage 1 kV, WD 3 mm, in-lens detector (a, b, c) and 3.5 kV, WD 4 mm, Everhart-Thornley detector (d).

of shrunk cells (results not shown). Since fixative diffusion into the cells is slowed down by cellular structures like cell walls, S-layers and extracellular polymers, it can vary with different strains and even from cell to cell, depending on cell size and geometry. Therefore, the fixation times used in this study may not necessarily be suitable for other specimens. Calculation of the diffusivity of formaldehyde in water, as done by Start et al. (1992), yielded times on the order of several minutes for diffusion to the center of a cell of micrometer size. Others have suggested using 30 min for formaldehyde fixation of prokaryotic cells (Braet et al. 1997).

Lower concentrations than the so-called half-strength Karnovsky solution (Karnovsky 1965; Kiernan 2000) (a solution of 2% glutaraldehyde and 4% formaldehyde in PBS) did not result in sufficient fixation of cells within reasonable times (results not shown). Many cells were removed during sample washing (after the fixation step) with only some organic remnants visible. Thus the half strength Karnovsky solution was used for all further experiments.

In order to fix many samples at once in a concise setup, samples can be turned upside down and put directly on the surface of fixative droplets instead of immersion into fixative placed in microtiter plate wells. Less fixative is needed and the sample processing is fast. In some cases, however, part of the sample material on the upside-down grids washed away from the grid and remained in the liquid when immersed into the liquid droplet. In this case, rendering the sample holder grid more hydrophilic by glow discharge (surface ionization that increases hydrophilicity) before placing the sample on the grid may help, as described by Aebi and Pollard (1987).

Glutaraldehyde fixation of microbial cells requires molecular oxygen due to glutaraldehyde-amine reactions during the cross-linking process leading to pyrimidines (Johnson 1987). When preparing samples of cultures which contain compounds that are sensitive to oxygen, such as Fe(II) minerals or adsorbed Fe(II), molecular oxygen can oxidize the Fe(II) within a few minutes to a few hours (in a strongly pH-dependent reaction) (Stumm and Morgan 1996). Although it is likely that the surface of the minerals will be slightly modified during this time, visually there was no difference between minerals in fixed and untreated samples. The analysis of surfaces of cell-mineral aggregates was therefore not affected. However, glutaraldehyde fixation should not last longer than 30 min in order to minimize the formation of secondary minerals.

Sample Preparation Step II: Dehydration. Sequential exchange of water by an organic solvent after chemical fixation of the samples is necessary since the water in the sample is not miscible with (and can therefore not be replaced by) liquid CO_2. We therefore examined the dehydration of geomicrobiological SEM samples using ethanol, acetone, or isopropanol with no difference to be observed between these solvents, suggesting that they are all equally suited for the dehydration of microbiological specimens. Since it is less of an irritant than acetone and also slightly less volatile than ethanol, we used isopropanol for our further studies and tested different treatment periods and solvent concentrations. Alcohols such as isopropanol have a much lower surface tension than water. Since they evaporate faster than water, the risk of samples drying out during sample handling is higher and more care has to be taken to avoid solvent evaporation and thereby drying of the samples.

For microbial cells of a few micrometers in diameter, we observed no difference in cell preservation (i.e., shape, size and surface structure of cells) when decreasing the time for dehydration from 15 min initially to just 20 s per step (results not shown), although differences in internal ultrastructure preservation most likely will occur. However, since we are only interested in the characterization of the surfaces and interfaces of the cell-mineral aggregates, we recommend using isopropanol for dehydration with dehydration steps of 20–60 s. However, the last step in pure solvent should not be shorter than 20 min in order to guarantee that complete dehydration of the samples is achieved. The short dehydration times utilized here are suitable for the small specimens used and for the examination of external structures to which this study aims. For larger specimens or ultrastructural analyses, the treatment duration would have to be adjusted accordingly. Generally, many dehydration steps of just slightly increasing concentrations are to be preferred in order to keep the solvent concentration gradients low.

When preparing SEM samples of cell-iron-mineral aggregates from phototrophic Fe(II)-oxidizing bacteria, we observed difficulties during the dehydration step with the purple-sulphur bacterium *Thiodictyon* sp. strain F4 that contains gas vacuoles. This strain lost its gas vacuoles in solutions of ethanol, acetone, or isopropanol at solvent concentrations exceeding 30% (not shown). Even dehydration via several sequential steps providing low gradients of organic solvent with respect to water could not eliminate this problem completely. Since critical point drying is not possible without dehydration, this implies that imaging of well preserved gas-vacuole containing cells would be possible only via light microscopy, environmental scanning electron microscopy (accepting the lower resolution available), or embedding the cells in a resin (that stabilizes the vacuoles before drying), thin-sectioning, and visualization via transmission electron microscopy (TEM). This was done by Cohen-Bazire et al. (1964) for comparison of the structures of gas vacuole-containing cells including a *Thiodictyon* strain. Additionally, SEM of cryofixed specimens could possibly be another technique to maintain and visualize gas vacuoles in microbial cells, since the surrounding matrix could potentially be stabilized in a frozen state preventing collapse of the vacuole structures.

Sample Preparation Step III: Critical Point Drying. After chemical fixation of the biological structures and replacement of the water by isopropanol, the sample can be dried completely by (i) replacing the organic solvent with liquid CO_2 under high pressure, (ii) increasing pressure and temperature above the critical point of CO_2, where it fills the chamber like a gas, but at its liquid density and (iii) releasing the pressure from the supercritical CO_2 leaving behind the dried sample with the preserved organic structures.

However, three factors have to be considered: first, before starting to heat the sample in the critical point drying device, the organic solvent should theoretically be completely replaced by liquid CO_2. Since the subsequent steps of introducing CO_2 and releasing half of the mixture of CO_2 and alcohol dilute the alcohol stepwise, 10 steps are required to reduce the organic solvent content to a concentration of significantly less than 0.1%. Secondly, during these 10 subsequent steps the pressure must not be allowed to drop significantly, otherwise the CO_2 will start to boil leading to sample destruction. The pressure should be readjusted frequently during the release in order to assure that the CO_2 is kept in its liquid state. Finally, the release of pressure from the supercritical CO_2 needs to be slow enough to keep the CO_2 gaseous or supercritical. A quick release will cool the medium faster, which can destroy the sample.

The critical point drying method is most suitable when high quality images are required (Beveridge and Graham 1991; Holt and Beveridge 1982). CPD leads to cells that are well prepared and not covered by remnants of growth medium or ice crystals. However, preparation artifacts can occur during sample preparation since the chemical fixation and dehydration by organic solvents obviously changes the chemistry in the direct cell environment and at the mineral surface. Also, chemical fixation usually requires oxygen, potentially leading to artifacts when dealing with oxygen-sensitive minerals. For this reason, the cryo-immobilization method was tested for some of the samples containing cell-mineral aggregates for a comparison to CPD prepared cells.

Preparation of Geomicrobiological Samples for Scanning Electron Microscopy via Cryo-Immobilization

In order to avoid artifacts from sample fixation and dehydration, different cryo electron microscopic techniques imaging frozen samples can be used. The approach chosen in this study resembles the method described by Erlandsen et al. (2003) with the differences that (i) our protocol did not include chemical fixation prior to freezing and (ii) no subsequent embedding via freeze-substitution was performed. In our experiments, the holey carbon coated TEM grids were taken directly out of the culture, rinsed with PBS and water, dried from below using filter paper, immersed into liquid nitrogen, transferred to the microscope in a cooled shuttle under nitrogen atmosphere and imaged at

temperatures of about −150°C. Where necessary, the samples were freeze-etched at −90°C for 5 min in order to remove small ice crystals which precipitated at the surface of the sample and coated with approximately 5 nm of tungsten.

SEM images of frozen samples confirmed the results obtained from critical point dried samples (Figure 2d): both CPD-prepared samples and cryo-immobilized samples showed tight associations of the cells with the minerals without the cells being encrusted in the iron minerals. Moreover, cell size, cell surface structure and the mineral shape seem to be the same. Immobilization of cell-mineral aggregate samples by immersion into liquid nitrogen is a very quick preparation method, and obviously produces no preparation artifacts that can be observed at the cell surface at SEM resolution (although not excluding potential artifacts concerning the ultrastructure of the cells). Thus, it potentially provides images that represent the closest to natural state possible for a scanning electron microscopy sample. The single steps that need to be carefully followed in order to obtain well preserved cryo-immobilized samples are washing, removal of excess water, rapid freezing, transport in the frozen state in a cooled shuttle into the electron microscope, and coating.

Washing. Samples for cryo-SEM need to be washed before freezing in order to prevent crystallization of growth medium remnants (i.e., salts, organic exudates, etc.) that would lead to the masking of structures of interest. Washing was optimal when the sample grids were slowly moved around for just a few seconds in three successive wells on a microtiter well plate, each filled with sterile-filtered bi-distilled water. Extensive washing damaged cells due to osmotic pressure acting on the cell surface and even washed cells away, whereas less washing resulted in a disturbance of the imaging by precipitated remnants of the growth medium.

Removal of Excess Water. Removal of water from the washed samples is the crucial step during cryo sample preparation. Complete removal dries the samples and destroys them due to the surface tension of the water and the loss of structural water from the cells. On the other hand, leaving too much water on the sample results in a larger specimen heat capacity, thus increasing the time required for cooling and the risk of ice crystal formation. Moreover, the opaque ice cover would require long times of freeze etching to make the sample accessible for imaging by the electron beam.

We successfully tested the removal of water by carefully touching the bottom and the edges of the sample with a piece of filter paper and leaving only a very thin film on the sample. The water present in the space between the copper rods always partially remained, thereby leaving only parts of the sample area free of disturbing water and thus accessible for imaging. However, we were unable to remove more of the water to increase the accessible sample area without damaging the cells. Therefore, we recommend testing different sample holders (different grids) which potentially allow fast removal of water without removing too much of the sample or without leaving too much remaining water.

Rapid Freezing. Vitrification of sample water by immersion into liquid N_2 is only fast enough for very small samples, as cooling times increase with the mass of the sample that needs to be cooled. For the micrometer sized samples examined in this study, heat transfer is governed by the convection of heat from the surface – the heat conductivity of the sample is negligible. A detailed description of the theory is given in Riehle (1968). Only more complex instrumental setups, e.g. for high-pressure freezing (Shimoni and Mueller 1998; Walther 2003; Zechmann et al. 2005) or propane jet freezing (Kaech and Woelfel 2007), make it possible to vitrify larger samples (up to and even >100 μm) and are widely used for the preparation of biological tissue for electron microscopy, as described already more than 20 years ago by Mueller and Moor (1984). Since our specimen are much smaller, the high cooling rates necessary to obtain vitrified samples are already achieved using plunge freezing. Thus, the application of technically challenging and expensive high pressure freezing used for larger specimens was not necessary and is therefore not included in this study.

We consider microbiological samples placed on TEM grids to be ideal for rapid freezing, since the latter are small, have a high surface area and are easy to handle with tweezers. As shown above, our experiments demonstrated that cryo-immobilization successfully avoided artifact formation when the TEM grid with the cell-mineral aggregates is placed directly in liquid nitrogen. Two important requirements make this very simple freezing technique work: (i) the tweezers with which the grid is handled need to be as thin as possible, as they can transfer heat to the sample and (ii) the samples have to be immersed in the liquid N_2 as fast as possible, since high turbulence around the cooled sample increases the cooling rate as more cryogen passes the surface per time.

Coating of CPD-Prepared and Cryo-Immobilized Samples

Coating is oftentimes required for both critical point-dried as well as cryo-immobilized samples, since biological material is neither very conductive, nor does it yield a high amount of secondary electrons for imaging. A thin metal layer provides the specimen with electrical conductivity, which avoids surface charging, and with increased secondary electron yield and, consequently, better signal-to-noise ratio. The coating layer should be as thin as possible (typically ∼5 nm) in order to maintain detailed surface structures, but thick enough to provide the sample with good conductivity.

For the present study, we analyzed more than 100 geomicrobial specimens and found that different geomicrobiological samples required different coating thicknesses in order to obtain good conductivity. Imaging of cell-mineral aggregates was facilitated by small particle sizes, the presence of particles that already showed sufficient conductivity before coating (e.g., iron minerals), large contact areas between the particles and the grid and optimal positioning of the particle on the grid (i.e., lying directly on the copper grid rather than the

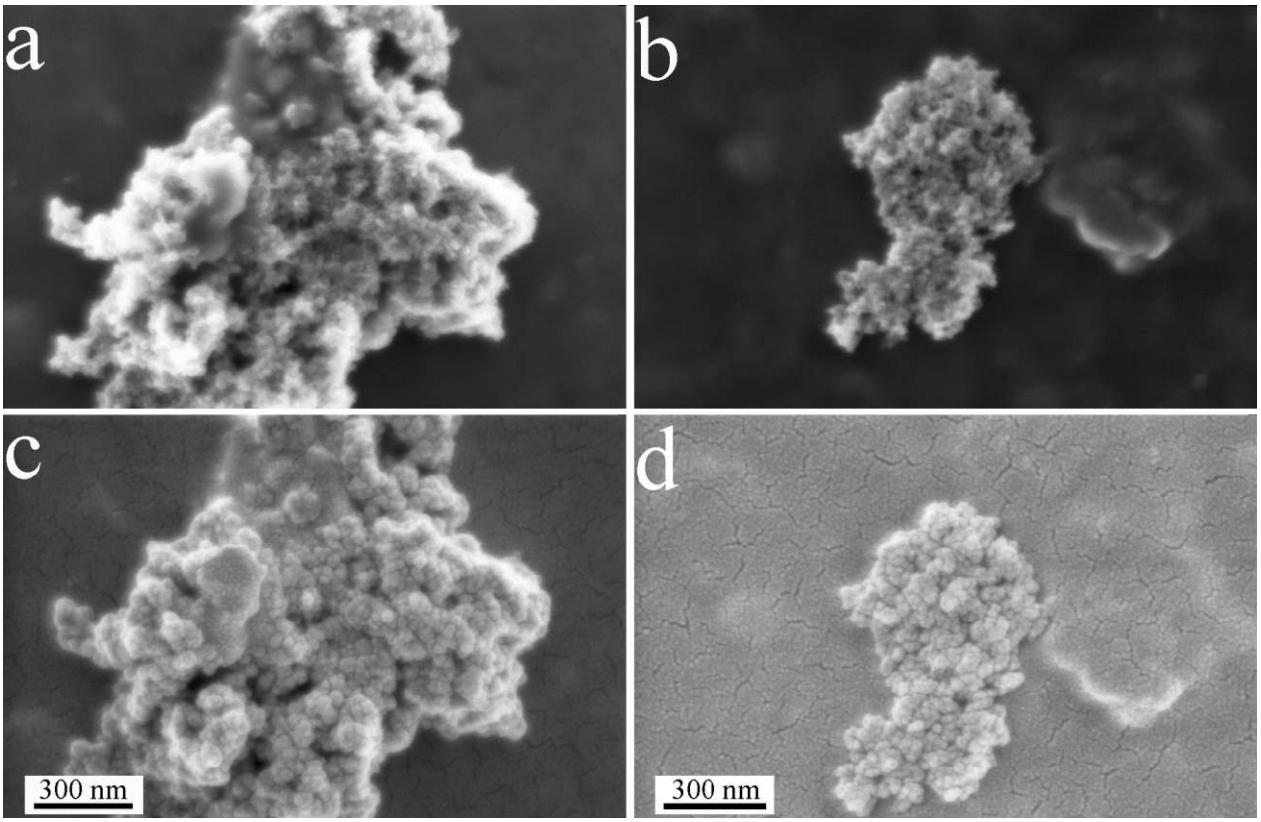

FIG. 3. Iron hydroxide (ferrihydrite) particles from cultures of the Fe(III)-reducing strain *Shewanella oneidensis* strain MR-4 growing on ferrihydrite. Images (a) and (b) show the uncoated particles. Micrographs (c) and (d) show the same particles after gold coating. Note the better material contrast relative to the background with uncoated particles. Imaging parameters: Acceleration voltage 2 kV, WD 4 mm, in-lens detector.

carbon film). The fewer of these sample requirements are fulfilled, the more important coating becomes in order to obtain samples that can be imaged without surface charging. Thus, the most suitable geomicrobiological samples are so conductive that the resolution which can be achieved without coating is on the order of the coating structures or better, thereby rendering coating unnecessary to achieve optimal results. Figure 3 shows microbially transformed iron minerals (from a culture of *Shewanella oneidensis* strain MR-4, growing on 30 mM ferric hydroxide) with and without gold/platinum (80%/20% w/w) coating.

Images in Figures 3a and 3b show the uncoated particles at the maximum of the achievable resolution (∼100,000 on the microscope's screen, ∼40,000 in the figure printed here); at higher magnification, surface charging makes imaging impossible. Figures 3c and 3d show the same particles after coating (at the same magnification). Imaging would be possible at a 10 times higher resolution after coating, but this only reveals the details of the coating layer, as the coating hides the material contrast between the mineral and the background and even masks some of the original sample features seen in Figures 3a and 3b. Therefore, depending on the surface structures of interest, coating can lead to masking of structures and misinterpretation. We therefore recommend to avoid coating whenever it is possible to image samples at acceleration voltages as low as 1 kV and less.

In our study, for critical point dried specimen, we used the rotary shadowing technique for coating, which has been described to be superior to unidirectional coating (Walther and Mueller 1999), and usually obtained good results. However, in the case of problems occurring due to remaining poor conductivity, masking of sample features by the coating material or radiation damage to the specimen, the application of an optimized double layer coating technique, as proposed by Walther et al. (1995), may provide a solution.

Cryo-immobilized samples were coated for imaging with thin tungsten layers of ∼5 nm thickness. Coating is done in the sample preparation stage and can be performed during the freeze etching process. The sample needs to be immediately transferred to the microscope after coating, since precipitation of moisture from the gas atmosphere in the shuttle can otherwise slowly cover the coated sample surface leading to poor imaging. Coating was necessary for all of our cryo-immobilized samples, as the electrical conductivity was very poor.

Comparison of CPD vs. Cryo-Immobilization of Geomicrobiological Samples

When comparing critical point drying (CPD) to cryo-immobilization of geomicrobiological samples, cryo-immobilization has two obvious advantages: it is very fast and it minimizes the risk of preparation artifacts. In practice, for some samples it turned out to be rather difficult to obtain high-resolution images of the cryo-immobilized samples since the reduction of the water film on the samples before freezing was difficult (for the reasons described earlier).

In many cases, however, we were successful in removing the water and the images of the cryo-immobilized cell-mineral aggregates showed the same spatial associations of cells and minerals that were observed when samples were prepared by critical point drying. Thus, the main conclusion for SEM imaging of geomicrobiological samples is that properly performed critical point drying does not alter the samples' surfaces. This is in contrast to what was previously reported by Montesinos et al. (1983), who had fixed their samples by 3% glutaraldehyde and stained them by osmium tetroxide after harvesting them by centrifugation. They found that bacterial cells (and especially phototrophic ones) shrank by an average factor of 2.3 during CPD sample preparation for SEM, due to pigment extraction by organic solvents during the dehydration process.

Imaging of Geomicrobiological Samples: Electron Microscope Parameters

Choosing appropriate acceleration voltages, working distances and detectors is of high importance if high resolution images of cell surfaces are to be obtained. The quality of electron micrographs and the information that they contain depend to a large extent on imaging parameters. The most important parameters and how we adjusted them are described below. Besides adjusting these parameters for every sample, we adjusted the focus and the stigmator coil voltages for every image in order to increase resolution. A constant aperture of 30 μm was used, since the microscopes were optimized to this setting.

Acceleration Voltage. The interaction volume of the primary electron beam with the specimen in the electron microscope gets larger with increased energy of the electrons. This causes secondary electron emission from a wider area of the sample surface and from greater sample depth. In this case, an image obtained from secondary electrons yields less information about the surface structure, but more information on the inside of the sample (e.g., up to the range of micrometers for these samples at 20 kV, following Kanaya and Kawakatsu 1972)) – at lower resolutions. Therefore, when the surface structure is analyzed, it is desirable to keep the acceleration voltage as low as possible.

Besides reducing the interaction volume between the primary electron beam and the sample, this also increases the relative secondary electron yield. Imaging at acceleration voltages below 5 kV is commonly referred to as "low voltage microscopy" and has been described in detail by Joy and Joy (1996). However, using low voltages also has some disadvantages including (i) longer scanning times, due to the lower secondary electron yield, (ii) lower resolution, since the electron beam is not well focused at large working distances, (iii) a lower contrast of topology and a lower contrast of different elements as a result of the lower specific secondary electron yield, and (iv) greater radiation damage to the sample due to the initial energy being dissipated in a small sample volume. As mentioned, a double layer coating can provide a solution to this latter problem (Walther et al. 1995).

Combinations of acceleration voltage and high vacuum in the sample chamber can be found where the sample charging, due to inflow of primary electrons into the sample, is at least partly compensated by emission of secondary electrons and gaseous ions (Cazaux 1999; Thiel et al. 2004). At these specific settings, high-resolution images can be obtained with uncoated samples. However, it is very time-consuming to determine this particular voltage (at a fixed given pressure), and during this process, biological samples are likely to be damaged by radiation or contaminated by hydrocarbons in the microscope's sample chamber. The latter are polymerized by the electron beam irradiation, building up a thin amorphous film on the sample.

Therefore, we determined the optimal acceleration voltage for each sample by searching for the highest resolution obtainable for one given particle of a specimen and then applied this acceleration voltage for the complete imaging session of the sample. An example for the effect of different acceleration voltages on the image quality is shown in Figure 4. The surface of the chemically fixed and critical point dried cell of the *Thiodictyon* sp. strain F4 can be seen best at voltages around 0.75–1 kV, whereas lower voltages lead to a poorly focused beam (resulting in a lower resolution and fuzzy images, see Figure 4a) and at higher voltages the surface information is hidden for the reasons described earlier in this section (Figures 4e, 4f, 4g, 4h). Generally, for our setup of samples and microscopes, $\sim$1 kV was observed to be optimal. We also have to note that the optimum acceleration voltage does not only depend on the sample and sample preparation, but also on the type of SEM and the tuning of the SEM.

Detectors. Two different types of detectors were compared: a standard Everhart-Thornley secondary electron (SE) detector in the sample chamber, and an improved in-lens detector, which is placed above the objective electron lens in the column of the microscope, thus detecting only the electrons that originate from the impact of the primary electron beam. Use of in-lens detectors yielded a better resolution due to the better signal-to-noise ratio of this detector type. The common SE detector had an overall higher signal than the in-lens detector and was less sensitive to surface charging of the sample. Therefore, whenever possible, in-lens detectors were used in this work for higher resolution. However, when surface charges get too disturbing, the use of common SE detectors is more convenient, in particular for uncoated samples. An example for the differences obtained by these two detectors is given in Figure 5, where the same

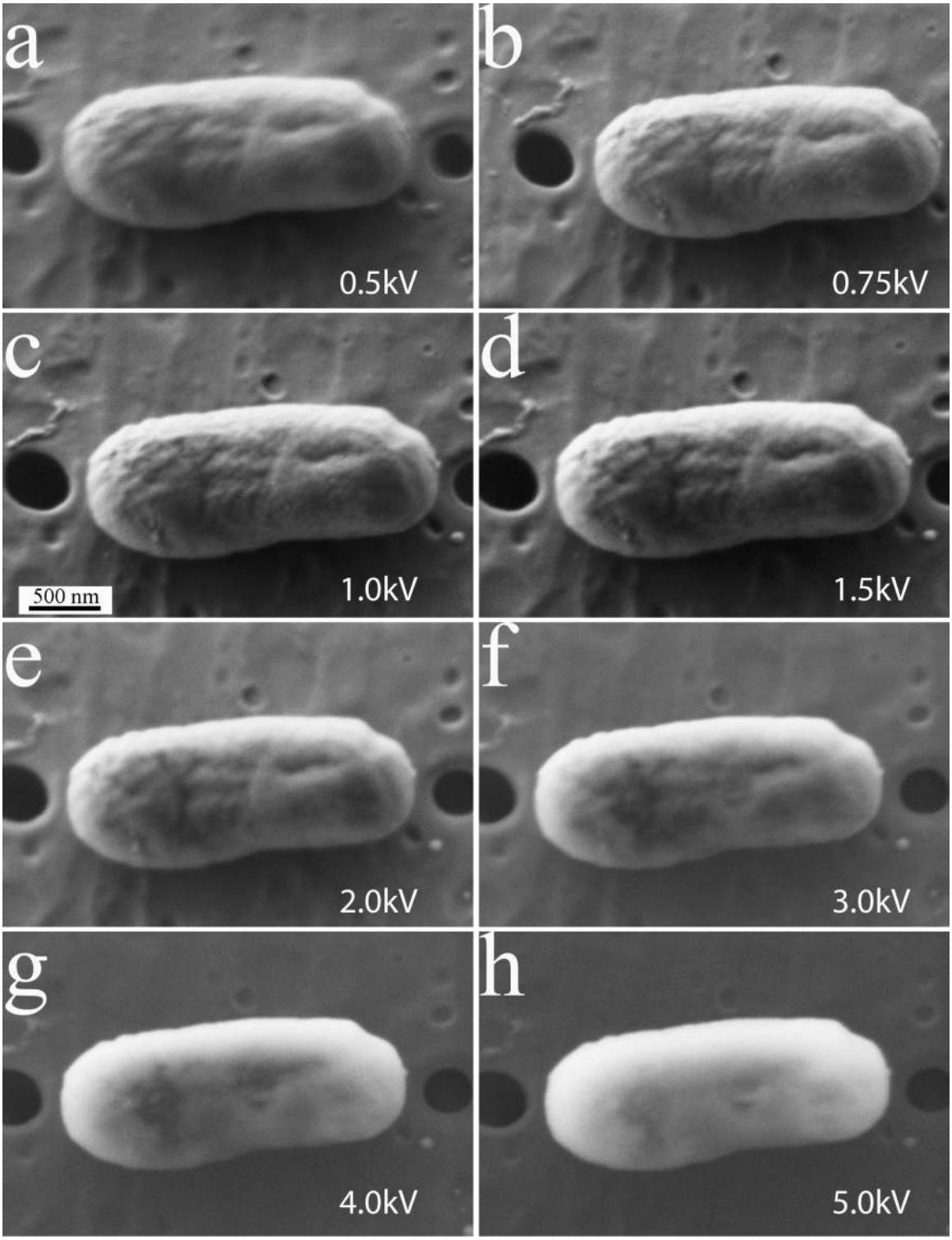

FIG. 4. Uncoated cell of the Fe(II)-oxidizing purple sulphur bacterium *Thiodictyon sp*. strain F4 after CPD, at different acceleration voltages. Imaging of the cell surface fine structure is optimal around 1.0 kV. Imaging parameters: WD 3 mm, Everhart-Thornley detector.

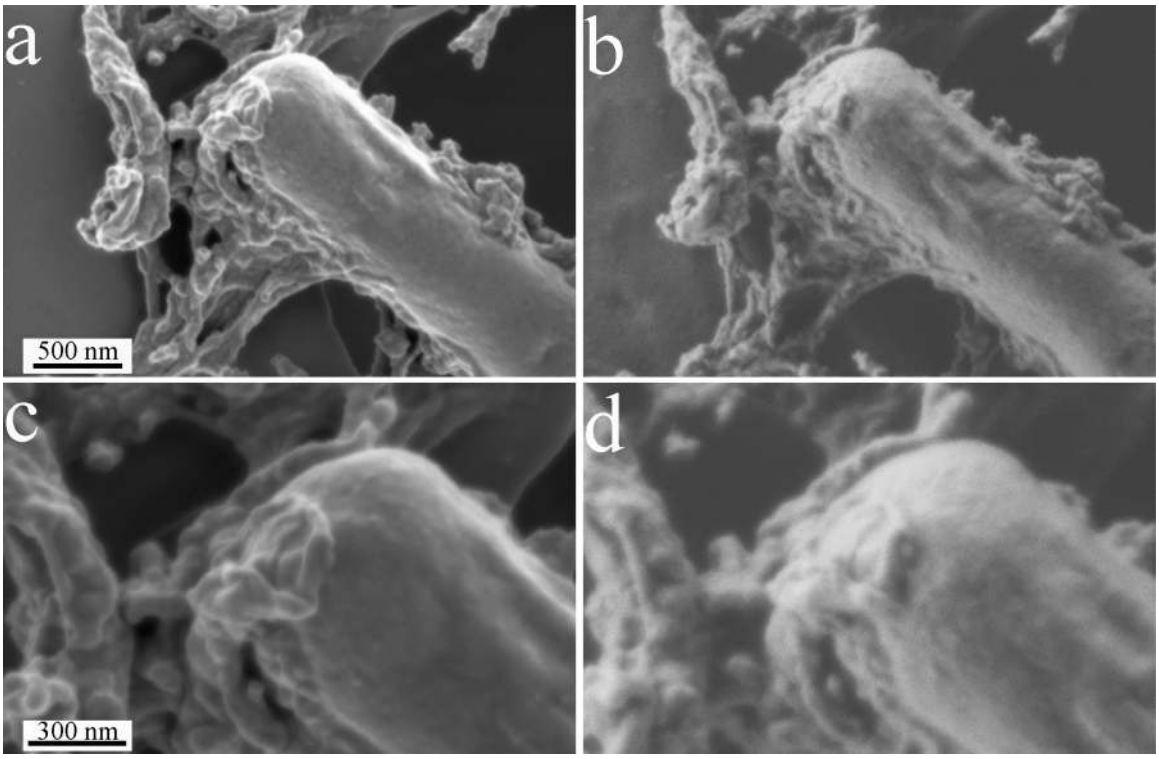

FIG. 5. Images of a critical point dried cell of the purple sulphur bacterium *Thiodictyon sp*. strain F4, without coating, using different detectors. Image (a): In-Lens detector; (b): SE2 detector. (c) and (d) are close-ups of (a) and (b), respectively. Imaging parameters: WD 1 mm, acceleration voltage 1.0 kV.

cell of *Thiodictyon* sp. strain F4 has been imaged with the two different detectors: the in-lens detector provides more detailed surface information than the standard SE detector.

Working Distance. The working distance is the distance between the specimen and the objective electron lens of the microscope column. Working distances generally need to be kept as small as geometrically possible, since longer beam travel leads to larger effects of electron lens errors. This can be limiting when samples with a complex geometry and large topography are imaged, or when samples are to be imaged at different angles.

Our EM analyses showed that, especially for the lowest acceleration voltages (in the range of 1 kV) that are preferred for uncoated samples in order to avoid charging effects, the working distance is a crucial parameter for obtaining high resolution. Decreasing the working distance will increase the resolution, but at the same time, it will also decrease the depth of field. This, however, is a problem only for samples with a pronounced topology, which was not the case for our samples.

CONCLUSIONS

Geomicrobiological samples, similar to biological samples, provide a challenge for electron microscopists as both sample preparation and imaging need to be carefully adjusted to this combination of wet and solid materials, which are susceptible for changes during sample preparation, have poor secondary electron yields and show low conductivities. In this study, we evaluated different methods for an optimized examination of the surface structure of such geomicrobiological samples. Based on our findings, we suggest the following as a general set of guidelines to consider when imaging geomicrobiological samples of comparable size and geometry:

1. For preservation of microbial cells, the samples should be chemically fixed for CPD. We observed no difference in cell preservation between successive and simultaneous formaldehyde and glutaraldehyde treatment.
2. Coating should be avoided whenever possible. Coating by conductive metal layers clearly facilitates imaging, but also reduces the resolution by masking regions of interest in many cases.
3. In case the sample surface is the research target, the microscope acceleration voltages need to be kept as low as possible, especially for non-coated samples. Suitable acceleration voltages necessary for high-resolution imaging vary for different samples and SEM working distances.

From the comparison of different preparation methods and from the evaluation of various imaging parameters we conclude that the preparation method of choice, as well as the optimal imaging parameters (choice of detector, acceleration voltage, working distance) vary for different samples and depend on the questions the researchers pose. In general it can be stated that simple rapid freezing techniques can serve as a standard for cell

preservation that is the closest possible to the natural state of cell-mineral aggregates.

Since high-resolution images are more difficult to obtain by cryo-SEM and the machinery necessary for cryo-SEM is expensive and requires experienced operators, we recommend CPD as a standard method for geomicrobiological sample preparation — if possible accompanied by control experiments using a cryo-SEM.

REFERENCES

Aebi U, Pollard TD. 1987. A glow discharge unit to render electron microscope grids and other surfaces hydrophilic. J Electron Microsc Techn 7:29–33.

Anderson TF. 1950. The use of critical point phenomena in preparing specimens for the electron microscope. J Appl Phys 21(7): 724.

Beveridge TJ, Graham LL. 1991. Surface layers of bacteria. Microbiol Rev 55(4):684–705.

Braet F, De Zanger R, Wisse E. 1997. Drying cells for SEM, AFM and TEM by hexamethyldisilazane: a study on hepatic endothelial cells. J Microsc 186 Pt 1:84–87.

Brown DA, Beveridge TJ, Keevil CW, Sherriff BL. 1998. Evaluation of microscopic techniques to observe iron precipitation in a natural microbial biofilm. FEMS Microbiol Ecol 26:297–310.

Cazaux J. 1999. Some considerations on the secondary electron emission, δ, from e– irradiated insulators. J Appl Phys 59:1418–1430.

Cohen-Bazire G, Pfennig N, Kunisawa R. 1964. The fine structure of green bacteria. J Cell Biol 22:207–225.

Ehrlich L. 1996. Geomicrobiology (3rd ed). New York: Marcel Dekker. 393 p.

Emerson D, Weiss JV. 2004. Bacterial iron oxidation in circumneutral freshwater habitats: findings from the field and the laboratory. Geomicrobiol J 21:405–414.

Erlandsen S, Lei M, Martin-Lacave I, Dunny G, Wells C. 2003. High resolution cryo SEM of microbial surfaces. Microsc Microanal 9:273–278.

Fortin D, Ferris FG. 1998. Precipitation of iron, silica, and sulfate on bacterial cell surfaces. Geomicrobiology 15:309–324.

Fortin D, Langley S. 2005. Formation and occurrence of biogenic iron-rich minerals. Earth Sci Rev 72(1-2):1–19.

Hammel I, Anaby D. 2007. Imaging of zymogen granules in fully wet cells. Evidence for restricted mechanism of granule growth. Microsc Res Techn 70:790–795.

Hansel CM, Benner SG, Fendorf S. 2005. Competing Fe(II)-induced mineralization pathways of ferrihydrite. Environ Sci Technol 39:7147–7153.

Holt SC, Beveridge TJ. 1982. Electron microscopy: its development and application to microbiology. Can J Microbiol 28:1–53.

Jefferson KK. 2004. What drives bacteria to produce a biofilm? FEMS Microbiol Lett 236:163–173.

Johnson TJA. 1987. Glutaraldehyde fixation chemistry: oxygen-consuming reactions. Euro J Cell Biol 45(1):160–169.

Joy DC, Joy CS. 1996. Low voltage scanning electron microscopy. Micron 27 (3–4):247–263.

Kaech A, Woelfel M. 2007. Evaluation of different freezing methods for monolayer cell cultures. Microsc Microanal 13 (Suppl. 2):240–241.

Kanaya K, Kawakatsu H. 1972. Secondary electron emission due to primary and backscattered electrons. J Appl Phys 5(43):1727–1742.

Kappler A, Newman DK. 2004. Formation of Fe(III) minerals by Fe(II)-oxidizing photoautotrophic bacteria. Geochim Cosmochim Acta 68(6):1217–1226.

Kappler A, Schink B, Newman DK. 2005. Fe(III)-mineral formation and cell encrustation by the nitrate-dependent Fe(II)-oxidizer strain BoFeN1. Geobiology 3:235–245.

Kappler A, Straub KL. 2005. Geomicrobiological cycling of iron. Reviews in Mineralogy and Geochemistry 59:85–108.

Karnovsky MJ. 1965. A formaldehyde-glutaraldehyde fixative of high osmolality for use in electron microscopy. J Cell Biol 27:137A–138A.

Kiernan JA. 2000. Formaldehyde, formalin, paraformaldehyde and glutaraldehyde: what they are and what they do. Microsc Today 1:8–12.

Kolter R, Greenberg EP. 2006. Microbial sciences: the superficial life of microbes. Nature 441(2):300.

Konhauser KO. 2006. Geomicrobiology (1st ed). London: Blackwell. 444 p.

Lovley DR, Holmes DE, Nevin KP. 2004. Dissimilatory Fe(III) and Mn(IV) reduction. Adv Microb Physiol 49:219–286.

Montesinos E, Esteve I, Guerrero R. 1983. Comparison between direct methods for determination of microbial cell volume: electron microscopy and electronic particle sizing. Appl Environ Microbiol 45(5):1651–1658.

Mueller M, Moor H. 1984. Cryofixation of suspensions and tissue by propane-jet freezing and high-pressure freezing. In: Bailey GW, editor. Proc. 42nd Annual Meeting of the Electron Microscopy Society of America. San Francisco, CA: San Francisco Press. P 6–9.

Myers CR, Myers JM. 1994 Ferric iron reduction-linked growth yields of Shewanella putrefaciens MR-1. J Appl Bacteriol 76(3):253–258.

Nealson KH, Saffarini D. 1994. Iron and manganese in anaerobic respiration: environmental significance, physiology and regulation. Ann Rev Microbiol 48:331–343.

Riehle U. 1968. Die Vitrifizierung verdünnter wässriger Lösungen. Chemie Ingenieur Technik 5:213–218.

Sabatini DD, Bensch K, Barrnett RJ. 1963. Cytochemistry and electron microscopy. The preservation of cellular ultrastructure and enzymatic activity by aldehyde fixation. J Cell Biol 17:19–58.

Schwertmann U, Cornell RM. 2000. Iron Oxides in the Laboratory. 2nd ed. New York: Wiley.

Shimoni E, Mueller M. 1998. On optimizing high-pressure freezing: from heat transfer theory to a new microbiopsy device. J Microsc 192(3):236–247.

Start RD, Layton CM, Cross SS, Smith JHF. 1992. Reassessment of the rate of fixative diffusion. J Clin Pathol 45:1120–1121.

Straub KL, Benz M, Schink B, Widdel F. 1996. Anaerobic, nitrate-dependent microbial oxidation of ferrous iron. Appl Environ Microbiol 62(4):1458–1460.

Stumm W, Morgan JJ. 1996. Aquatic Chemistry, 3rd ed. New York: Wiley-Interscience. 1040 p.

Thiberge S, Nechushtan A, Sprinzak D, Gileadi O, Behar V, Zik O, Chowers Y, Michaeli S, Schlessinger J, Moses E. 2004. Scanning electron microscopy of cells and tissues under fully hydrated conditions. Proc Natl Acad Sci 101(10):3346–3351.

Thiel BL. 2006. Imaging and microanalysis in environmental scanning electron microscopy. Microchim Acta 155:39–44.

Thiel BL, Toth M, Craven JP. 2004. Charging processes in low vacuum scanning electron microscopy. Microsc Microanal 10:711–720.

Walther P. 2003. Recent progress in freeze-fracturing of high-pressure frozen samples. J Microsc 212(1):34–43.

Walther P, Mueller M. 1999. Biological ultrastructure as revealed by high resolution cryo-SEM of block faces after cryo-sectioning. J Microsc 196(3):279–287.

Walther P, Wehrli E, Hermann R, Mueller M. (1995). Double-layer coating for high-resolution low-temperature scanning electron microscopy. J Microsc 179(3):227–237.

Weber KA, Achenbach LA, Coates JD. 2006. Microorganisms pumping iron: anaerobic microbial iron oxidation and reduction. Nature Rev Microbiol 4:752–764.

Widdel F, Schnell S, Heising S, Ehrenreich A, Assmus B, Schink B. 1993. Ferrous iron oxidation by anoxygenic phototrophic bacteria. Nature 362:834–836.

Zechmann B, Mueller M, Zellnig G. 2005. Effects of different fixation and freeze substitution methods on the ultrastructural preservation of ZYMV-infected Cucurbita pepo (L.) leaves. J Electron Microsc 54(4):393–402.